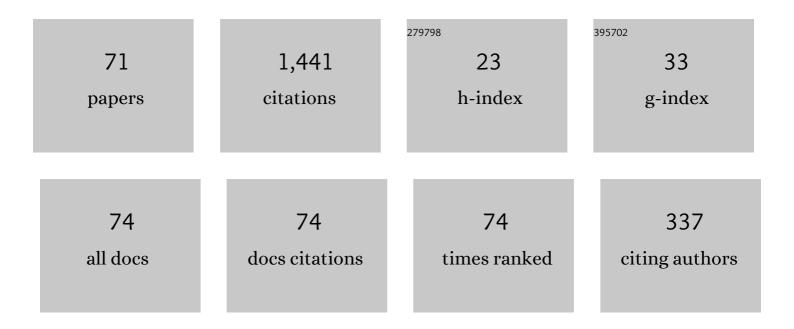
List of Publications by Year in descending order

Source: https://exaly.com/author-pdf/6542211/publications.pdf Version: 2024-02-01



#	Article	IF	CITATIONS
1	Possible improvements of alumina–magnesia castable by lightweight microporous aggregates. Ceramics International, 2015, 41, 1263-1270.	4.8	86
2	Slag Resistance Mechanism of Lightweight Microporous Corundum Aggregate. Journal of the American Ceramic Society, 2015, 98, 1658-1663.	3.8	68
3	Isolation or corrosion of microporous alumina in contact with various CaO-Al 2 O 3 -SiO 2 slags. Corrosion Science, 2017, 120, 211-218.	6.6	55
4	Corrosion of Al2O3–Cr2O3 refractory lining for high-temperature solid waste incinerator. Ceramics International, 2015, 41, 14748-14753.	4.8	50
5	Properties and microstructures of lightweight alumina containing different types of nano-alumina. Ceramics International, 2018, 44, 17885-17894.	4.8	48
6	Slag corrosion-resistance mechanism of lightweight magnesia-based refractories under a static magnetic field. Corrosion Science, 2020, 167, 108517.	6.6	46
7	Correlations among processing parameters and porosity of a lightweight alumina. Ceramics International, 2018, 44, 14076-14081.	4.8	45
8	Dynamic interaction of refractory and molten steel: Corrosion mechanism of alumina-magnesia castables. Ceramics International, 2018, 44, 14617-14624.	4.8	45
9	Effect of nano-alumina sol on the sintering properties and microstructure of microporous corundum. Materials and Design, 2016, 89, 21-26.	7.0	40
10	Design, fabrication and properties of lightweight wear lining refractories: A review. Journal of the European Ceramic Society, 2022, 42, 744-763.	5.7	38
11	Dynamic slag/refractory interaction of lightweight Al2O3–MgO castable for refining ladle. Ceramics International, 2015, 41, 8149-8154.	4.8	36
12	Effects of MgO micropowder on microstructure and resistance coefficient of Al2O3–MgO castable matrix. Ceramics International, 2014, 40, 7023-7028.	4.8	33
13	Enhanced corrosion resistance through the introduction of fine pores: Role of nano-sized intracrystalline pores. Corrosion Science, 2019, 161, 108182.	6.6	32
14	Effects of aggregate microstructure on slag resistance of lightweight Al2O3-MgO castable. Ceramics International, 2017, 43, 16495-16501.	4.8	31
15	Corrosion modeling of magnesia aggregates in contact with CaO–MgO–SiO ₂ slags. Journal of the American Ceramic Society, 2020, 103, 2128-2136.	3.8	31
16	Mathematical Modeling on Erosion Characteristics of Refining Ladle Lining with Application of Purging Plug. Metallurgical and Materials Transactions B: Process Metallurgy and Materials Processing Science, 2013, 44, 744-749.	2.1	30
17	Fabrication and analysis of lightweight magnesia based aggregates containing nano-sized intracrystalline pores. Materials and Design, 2020, 186, 108326.	7.0	30
18	Toward CFD Modeling of Slag Entrainment in Gas Stirred Ladles. Steel Research International, 2015, 86, 1447-1454.	1.8	29

#	Article	IF	CITATIONS
19	Fabrication and properties of in situ intergranular CaZrO3 modified microporous magnesia aggregates. Ceramics International, 2020, 46, 16956-16965.	4.8	28
20	Effect of MgO micropowder on sintering properties and microstructures of microporous corundum aggregates. Ceramics International, 2015, 41, 5857-5862.	4.8	27
21	Fabrication and characterization of lightweight microporous alumina with guaranteed slag resistance. Ceramics International, 2016, 42, 8724-8728.	4.8	27
22	Influence of pore distribution on the equivalent thermal conductivity of low porosity ceramic closed-cell foams. Ceramics International, 2018, 44, 19319-19329.	4.8	26
23	Corrosion mechanism of Al2O3–SiC–C refractory by SiO2–MgO-based slag. Ceramics International, 2020, 46, 28262-28267.	4.8	25
24	Characterisation and properties of low-conductivity microporous magnesia based aggregates with in-situ intergranular spinel phases. Ceramics International, 2021, 47, 11063-11071.	4.8	25
25	Slag corrosion mechanism of lightweight Al ₂ O ₃ –MgO castable in different atmospheric conditions. Journal of the American Ceramic Society, 2018, 101, 2096-2106.	3.8	24
26	Dynamic interaction of refractory and molten steel: Effect of alumina-magnesia castables on alloy steel cleanness. Ceramics International, 2018, 44, 22146-22153.	4.8	24
27	Fabrication of lightweight alumina with nanoscale intracrystalline pores. Journal of the American Ceramic Society, 2020, 103, 2262-2271.	3.8	24
28	Effects of particle distribution of matrix on microstructure and slag resistance of lightweight Al 2 O 3 –MgO castables. Ceramics International, 2016, 42, 1964-1972.	4.8	23
29	Towards chrome-free of high-temperature solid waste gasifier through in-situ SiC whisker enhanced silica sol bonded SiC castable. Ceramics International, 2017, 43, 3330-3338.	4.8	22
30	Corrosion mechanism of lightweight microporous aluminaâ€based refractory by molten steel. Journal of the American Ceramic Society, 2019, 102, 3705-3714.	3.8	21
31	Towards prediction of local corrosion on alumina refractories driven by Marangoni convection. Ceramics International, 2018, 44, 1675-1680.	4.8	20
32	Numerical Simulation on Refractory Wear and Inclusion Formation in Continuous Casting Tundish. Metallurgical and Materials Transactions B: Process Metallurgy and Materials Processing Science, 2021, 52, 1344-1356.	2.1	20
33	Towards slag-resistant, anti-clogging and chrome-free castable for gas purging. Ceramics International, 2016, 42, 18674-18680.	4.8	17
34	Corrosion of alumina-magnesia castable by high manganese steel with respect to steel cleanness. Ceramics International, 2019, 45, 9884-9890.	4.8	15
35	Computational Modeling and Prediction on Viscosity of Slags by Big Data Mining. Minerals (Basel,) Tj ETQq1 1	0.784314 ı 2.0	gBT /Overloc

An approach for matrix densification based on particle packing and its effect on lightweight Al2O3-MgO castables. Ceramics International, 2016, 42, 18560-18567.

4.8 14

#	Article	IF	CITATIONS
37	Enhancement of bonding network for silica sol bonded SiC castables by reactive micropowder. Ceramics International, 2017, 43, 8850-8857.	4.8	13
38	Incorporating Zr combined Si and C to achieve self-repairing ability and enhancement of silica sol bonded SiC castables. Journal of Alloys and Compounds, 2018, 732, 396-405.	5.5	13
39	Fabrication of lightweight alumina containing fine closed pores by controlling the relationship between phase stress and superplasticity: Experimental and mathematical studies. Ceramics International, 2018, 44, 20034-20042.	4.8	13
40	Novel phenomenon of quasiâ€volcanic corrosion on the alumina refractoryâ€slagâ€air interface. Journal of the American Ceramic Society, 2020, 103, 6639-6649.	3.8	13
41	Formation Mechanism of In Situ Intergranular CaZrO3 Phases in Sintered Magnesia Refractories. Metallurgical and Materials Transactions A: Physical Metallurgy and Materials Science, 2020, 51, 5328-5338.	2.2	13
42	Corrosion Behavior of Lightweight MgO in High Basicity Tundish Slag. Steel Research International, 2021, 92, 2100010.	1.8	13
43	Effect of lightweight refractories on the cleanness of bearing steels. Ceramics International, 2018, 44, 12965-12972.	4.8	12
44	Towards chrome-free lining for plasma gasifiers using the CA6-SiC castable based on high-temperature water vapor corrosion. Ceramics International, 2019, 45, 12429-12435.	4.8	12
45	A thermodynamic assessment of precipitation, growth, and control of MnS inclusion in U75V heavy rail steel. High Temperature Materials and Processes, 2021, 40, 178-192.	1.4	12
46	Mechanical performance and oxidation resistance of SiC castables with lamellar Ti3SiC2 coatings on SiC aggregates prepared by SPS. Journal of Alloys and Compounds, 2019, 791, 461-468.	5.5	10
47	Effect of Ti combined with Si and C on mechanical performance and oxidation resistance of SiC castables for plasma gasifier. Ceramics International, 2019, 45, 4147-4151.	4.8	10
48	Adsorption mechanism of oxide inclusions by microporous magnesia aggregates in tundish. Ceramics International, 2022, 48, 427-435.	4.8	10
49	Visual measurement and characterisation of quasi-volcanic corrosion at alumina ceramic-oxides melt-air interface. Journal of the European Ceramic Society, 2021, 41, 400-410.	5.7	10
50	Thickness monitoring and discontinuous degradation mechanism of wear lining refractories for refining ladle. Journal of Iron and Steel Research International, 2022, 29, 1110-1118.	2.8	10
51	Incorporating Zr to achieve self-protecting and enhancement of silica sol bonded SiC castables at active oxidation condition. Ceramics International, 2018, 44, 6089-6095.	4.8	9
52	Chemical interactions between a calcium aluminate glaze and molten stainless steel containing alumina inclusions. Ceramics International, 2018, 44, 1099-1103.	4.8	8
53	Role of liquid phase amounts in the pore evolution of lightweight bauxite: Experimental and thermal simulation studies. Ceramics International, 2019, 45, 6216-6222.	4.8	8
54	Corrosion resistance and antiâ€reaction mechanism of Al ₂ O ₃ â€based refractory ceramic under weak static magnetic field. Journal of the American Ceramic Society, 2022, 105, 2869-2877.	3.8	8

#	Article	IF	CITATIONS
55	Pore evolution of microporous magnesia aggregates with the introduction of nano-sized MgO. Ceramics International, 2022, 48, 18513-18521.	4.8	8
56	Computational Simulation and Prediction on Electrical Conductivity of Oxide-Based Melts by Big Data Mining. Materials, 2019, 12, 1059.	2.9	7
57	Comparison study on effect of nano-sized Al2O3 addition on the corrosion resistance of microporous magnesia aggregates against tundish slag. Ceramics International, 2022, 48, 5139-5144.	4.8	6
58	Improvement of Durability of Purging Plugs Using MgO Micropowder for Refining Ladles. International Journal of Applied Ceramic Technology, 2016, 13, 1104-1111.	2.1	5
59	Effect of magnesia-calcium hexaaluminate refractories on the quality of low-carbon alloy steel. Ceramics International, 2022, 48, 31181-31190.	4.8	5
60	The Interfacial Behavior of Alumina-Magnesia Castables and Molten Slag under an Alternating Magnetic Field. InterCeram: International Ceramic Review, 2018, 67, 36-43.	0.2	4
61	Improved bonding properties of rectorite clay slurry after wet/dry grinding. Applied Clay Science, 2019, 183, 105318.	5.2	4
62	Modified phenolic resin with aluminium and rectorite: Structure, characterization, and performance. Polymer Composites, 2020, 41, 4431-4441.	4.6	4
63	Enhancement of the densification and thermal properties of Ca2Mg2Al28O46 ceramic by MnO addition. Ceramics International, 2020, 46, 18734-18741.	4.8	4
64	Effect of carbon black on corrosion resistance of Al2O3–SiC–C castables to SiO2–MgO slag. Ceramics International, 2022, , .	4.8	4
65	Synthesis, characterization, visualization, and growth mechanism of macro-sized tubular MgO crystals formed in situ from refractory magnesia with aluminum. Ceramics International, 2022, 48, 23800-23807.	4.8	3
66	Corrosion Mechanism of Foamed Slag on the Lightweight Corundum-Spinel Castable. InterCeram: International Ceramic Review, 2016, 65, 226-231.	0.2	2
67	The Interfacial Behavior of Alumina-Magnesia Castables and Molten Slag under an Alternating Magnetic Field. InterCeram: International Ceramic Review, 2018, 67, 58-65.	0.2	2
68	Corrosion Mechanisms of Different Refractory Aggregates in Contact with SiO2-MgO-Based Slag. InterCeram: International Ceramic Review, 2020, 69, 22-29.	0.2	2
69	Study on a Lime-Fluorite Slag Melting Agent for Ladle Slag Buildup. InterCeram: International Ceramic Review, 2015, 64, 116-118.	0.2	0
70	Oxidation Resistance and Mechanical Enhancement of Ferro-Silicon Nitride on Silica Sol Bonded SiC Castable. Key Engineering Materials, 0, 768, 286-290.	0.4	0
71	Mathematical Simulation and Physical Modeling of Self-Source Magnetization by Liquid Electrolyte Flow. Materials Science Forum, 0, 982, 165-172.	0.3	0